DIGITAL MAGNETIC IMAGING OF STEEL CORD CONVEYOR BELTS IN PRACTICE

MJ Alport, JF Basson, AJ Fiddler and T Padayachee

1. INTRODUCTION

Steel cord reinforced conveyor belting is widely used for the transportation of various products (e.g. coal and ash in power stations), particularly for long overland conveyors. The ability to perform continuous non-destructive condition monitoring of these belts would be beneficial to improve the reliability and availability of these belt transport systems.

Although X-ray technology has been successfully employed for the online imaging of cord and splice defects in steel cord reinforced belting[[1]], the high cost of such systems combined with safety issues due to the radiation hazard discourages their use for permanent installations. Furthermore, there has been a voiced request for a system that continuously monitors cord damages which will both identify the location and severity (number of cord breaks) as well as give damage growth analysis so that maintenance can be more efficiently scheduled. Another alternative technique[2] that was developed in the 1980's measures the magnetic fringing fields that occur above breaks in previously magnetised cords. Initial implementations of this technology relied on relatively few sensors, and because these sensors were mostly coils, their output was proportional to the rate of change of the magnetic field. This signal, typically viewed on a chart recorder, was often difficult and ambiguous to interpret.

In March 2006, the development[3] of a new second-generation magnetic technology[4,5] commenced. This Digital Magnetic Imaging (DiMI) technology uses an array of magnetic field (*B*-field) sensors that measure the local value of the magnetic field directly, and can give a high-resolution image of belt damages and splices. A DiMI prototype was initially installed on the Phase 2 Incline Belt at New Denmark Colliery, South Africa in November 2007, and was subsequently upgraded in July 2008. Further DiMI units have been installed, under a license contract, by a large conveyor belt manufacturer in Brazil, Canada, Chile and Zambia. Features of these installations include real-time monitoring of cord damages with critical and non-critical alarm notification and on-demand reporting.

As with any new technology, the laboratory prototype must necessarily be exposed to a rigorous field testing schedule. This paper describes some of the lessons learnt from these initial tests.

Finally, wavelet filtering is briefly demonstrated as a signal processing tool to assist with solving problems encountered with current DiMI installations.

2. DESCRIPTION OF THE DIGITAL MAGNETIC IMAGING (DIMI) SYSTEM

DiMI uses digital magnetic imaging to obtain a high-resolution image of the magnetic anomalies that occur above the steel cords at damage locations in conveyor belts. The strength of the magnetic field depends on the structure of the cord damage and the belt-sensor distance. Typically, for distances of about 5cm from the belt, the magnetic field strengths above single cord breaks are only 1 to 5 times stronger than that of the Earth's field i.e. about 1 to 3 Gauss.

2.1 FRINGING MAGNETIC FIELD OF A BROKEN STEEL CORD

Figure 1 shows a schematic of the fringing magnetic field that forms above a broken magnetised cord together with a plot of the vertical component of the magnetic field strength. Due to the break, the left hand cord ends in a north pole and the right hand cord begins as a south pole. The plot at the bottom shows the vertical component of magnetic field, B_z, measured along the dashed line, *L*. The characteristic shape of this trace is typical of the signal that is detected by a magnetic field sensor placed above a running belt. Considering the trace from left to right, initially at *A*, B_z~0, i.e. there is no field above intact cords. At *B*, the vertical component of the field has increased and reaches a maximum. B_z then decreases to

zero in the centre of the break (between *B* and *C*) before decreasing to a minimum at *C*. Far away from the break, B_z again returns to zero. In summary, a damaged cord (either a partial or complete break) will result in a bipolar signal being detected by magnetic sensors placed above the belt.

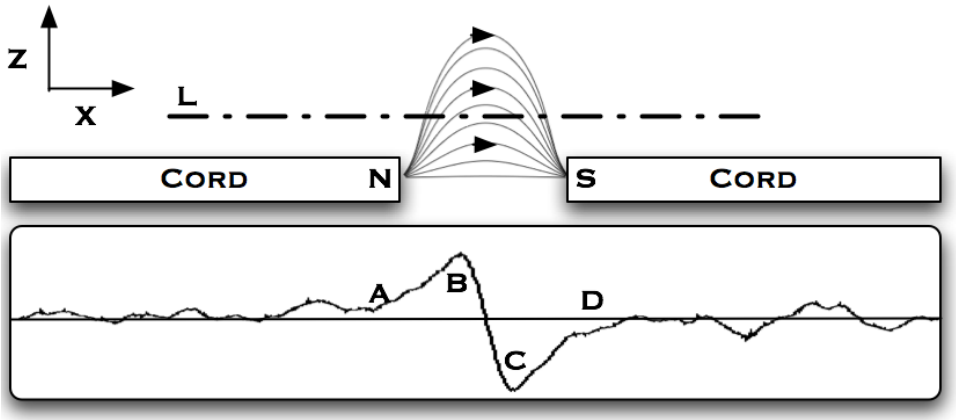

Figure 1: The top sketch shows the magnetic flux lines above the north and south poles of a cord break. The bottom plot shows the vertical *z*-component of the magnetic field, B_z, measured along the dashed line, *L*.

2.2 FUNCTIONALITY

DiMI provides continuous monitoring of steel cord reinforced conveyor belts. It uses magnetic imaging technology to capture the magnetic fringing fields above the conveyor belt, and then calculates the position and severity of the cord breaks from this data. The system is connected to the internet or a LAN that enables the customer to verify alarm events, upgrade the software and download on-demand reports.

2.3 SYSTEM CONFIGURATION

A typical arrangement of the DiMI-system is shown in **Figure 2**. The hardware components of DiMI are as follows: (1) Sensor, (2) Magnet, (3) CPU Box, (4) Power Supply Cabinet, and (5) Proximity Sensor.

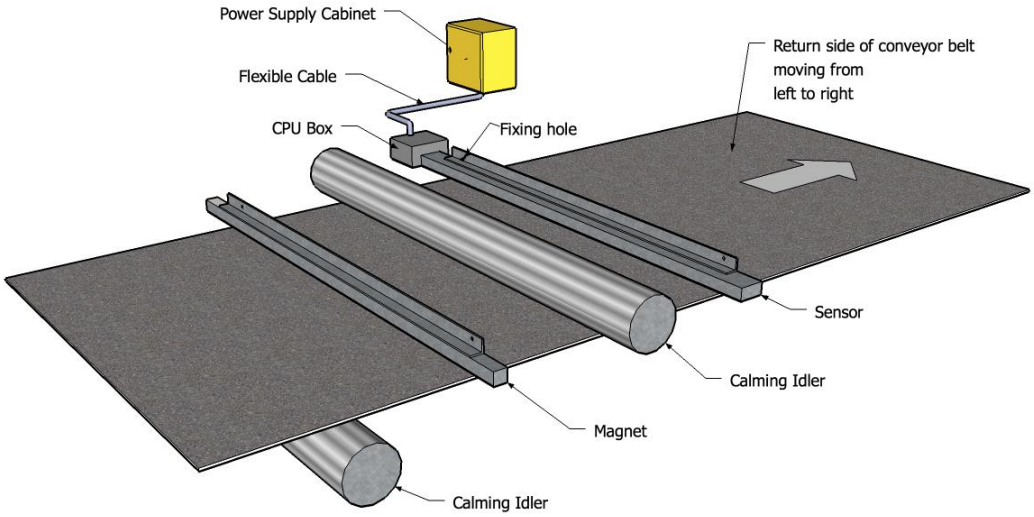

Figure 2: Schematic of a DiMI-monitoring system installed on a conveyor belt.

DiMI is installed on the flat, return side of the conveyor belt. The magnet is placed about 2m from straight calming idlers, just upstream of the sensor. The sensor, attached to the power supply cabinet, is placed about 2 to 4m downstream of the magnet. A proximity sensor (not

shown in **Figure 2**) is attached to a nearby pulley and used for positional information. An Ethernet cable attached to the CPU box can either be connected to a laptop, an internet modem (e.g. ADSL) or a LAN. Voltage-free relay contacts supply critical and non-critical alarm signals to the conveyor PLC.

3. CAPTURED DATA

Some examples of data captured by DiMI will now be presented. The belt schematic will be described and typical example images of splices and damages, collected from currently installed DiMI installations, will be shown.

3.1 BELT SCHEMATIC

Experience has shown that a typical belt user does not have the time or inclination to view magnetic data in its raw form, as presented in **Sections 3.2 & 3.3** below. As a result, a simplified presentation of the raw magnetic data, called the belt schematic, has been implemented. This belt schematic is a full view of the belt, showing identified splices and damages. A typical belt schematic is shown in **Figure 3**.

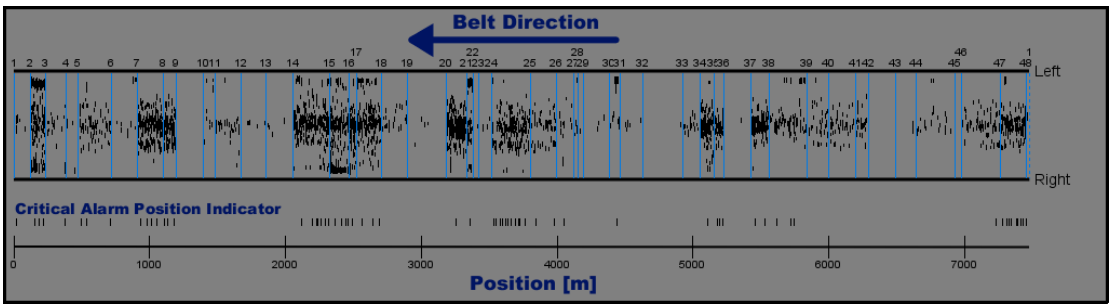

Figure 3: A typical belt schematic showing the splices and damages.

The top region shows the full belt width bounded by the two dark horizontal lines. The splices are marked by vertical lines and numbered along the length of the belt at the top. The damages are marked with vertical line segments. The positions of the damages are accurately represented on the schematic and the length of the line segments is proportional to the size of each damage. The position information obtained from the proximity sensor is shown at the bottom. The start of the belt is defined as the splice immediately following the shortest segment as would be the case for a new belt, and it is therefore not necessary to add any reference markers to the belt itself. Thus, the belt schematic gives a quick overview of the condition of the belt indicating which segments contain high levels of damage, and hence should be considered for repair and/or replacement.

The Graphics User Interface (GUI) of DiMI also allows the customer to zoom in and display the splices and/or damages in more detail. Some examples are given below.

3.2 SPLICES

Typical splice images recorded by DiMI can be seen in **Figure 4** below. The white and black regions of the image represent the north and south poles, respectively, of the cord ends in the spices. Specifically, **Figure 4(c)** also shows some cord ends and breaks on either side of the splice.

(a) **(b)** **(c)**

Figure 4: Typical images of splices recorded with DiMI: (a) Single-stage splice, (b) 2-Stage splice, (c) Modified 2-stage splice together with cord ends and breaks.

3.3 DAMAGES

Figures 5, 6 & 7 show examples of cord damage, edge cord damage as well as single cord ends. The fainter vertical stripes that span almost the full width of the belt are artefacts caused by belt vibration.

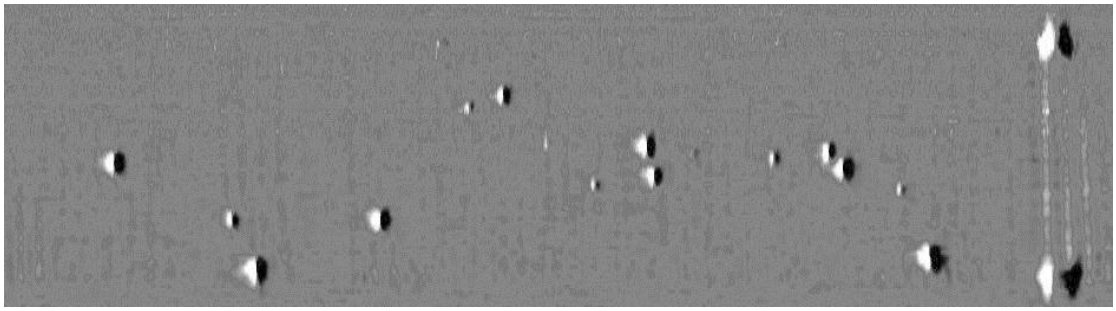

Figure 5: Magnetic image showing multiple cord damages in a region of a belt. Each damage can be identified by its characteristic bipolar signature, that is, a bright region followed by a dark region, representing the north and south poles. The size of the magnetic image of a damage is directly proportional to the physical size of the cord breaks.

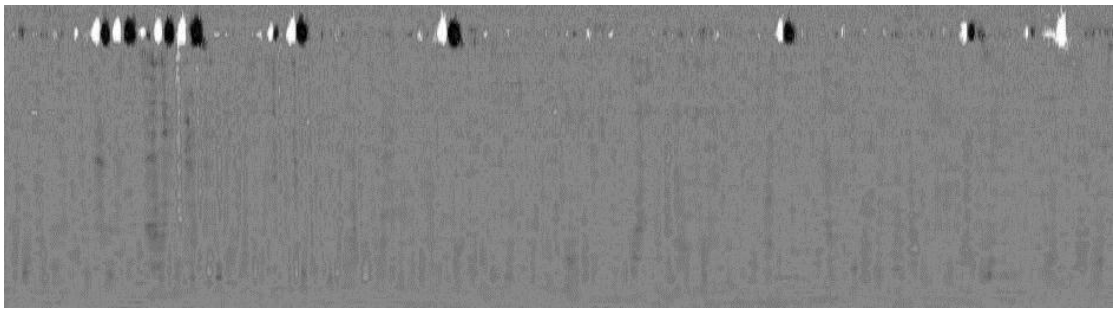

Figure 6: Magnetic image showing multiple edge damages to the belt, seen at the top of the image.

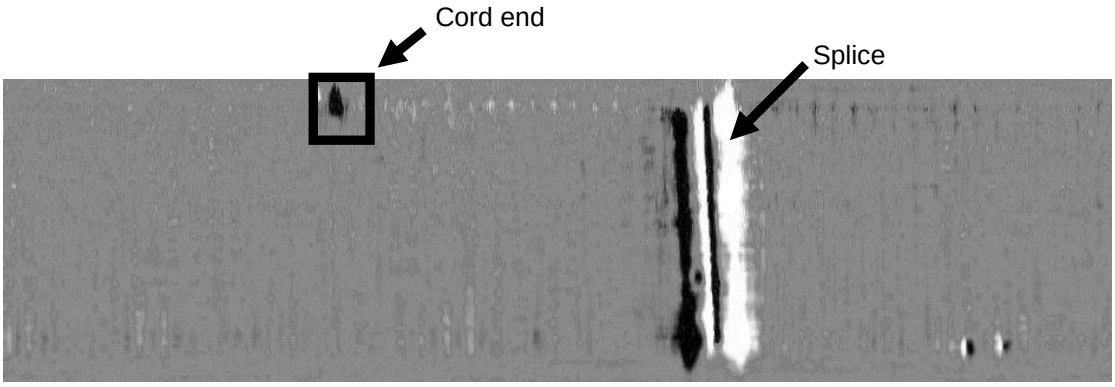

Figure 7: The region enclosed by the rectangle at the top left of the image shows an example of a cord end located at the edge of the belt. The end is black, implying a south pole. It is identified by the lack of a nearby bright region or north pole. In actuality, the north pole is located at the other end of the cord, which in this case terminates in the splice.

4. DIMI AT NEW DENMARK COLLIERY

In November 2007, a DiMI prototype was installed on the Phase 2 Incline Belt at New Denmark Colliery near Standerton, South Africa. The Phase 2 Incline Belt is rated at ST3150, 2.2km long, 1.35m wide and runs at a nominal speed of 4m/s.

In July 2008 the prototype was upgraded to satisfy the full technical specification, including an operating temperature range of -40°C to +70°C.

4.1 INTERNET ACCESS

During the development phase of the project, it was perceived that providing internet access to the DiMI units would offer significant advantages. Internet connectivity would allow for the monitoring of the unit's operational status and uploading of new firmware revisions as they become available. However, experience with installed sites so far has indicated that it is quite difficult for some sites to provide internet access, citing security as a concern.

Figure 8 shows a block diagram of the DiMI internet configuration at the New Denmark installation. A satellite-based internet connection was used instead of the more preferred ADSL technology as the site was too far from an exchange. 3G was also investigated but was found to be too expensive.

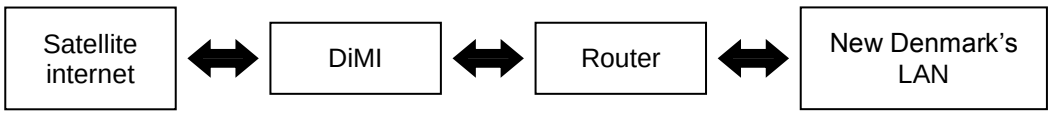

Figure 8: Block diagram showing the configuration of the internet access to the DiMI-unit installed at New Denmark Colliery.

Both New Denmark personnel and other internet users (provided they have the appropriate authorisation) can access the system. The router has a built-in firewall, ensuring there is no direct connection between the internet and the Colliery's LAN. Hence, there is no possibility of compromising the Colliery's IT security.

Although the satellite internet connection has been fairly reliable, on one occasion access was lost when the service provider changed the password without prior warning. The only other network-related problem involved a faulty network hub, which was subsequently replaced.

4.2 PROXIMITY SENSOR

The proximity sensor is an essential component of DiMI, and is responsible for providing belt positional information. Generally bolt heads, arranged just inside the circumference of a

nearby pulley, serve as suitable targets for the proximity sensor. As an alternative to the bolt heads, a spoked wheel, attached to a pulley shaft, has also been used.

At the New Denmark installation, falling coal debris has, on at least one occasion, dislodged the proximity sensor, resulting in spurious pulse data. Consequently, the positions of belt splices were being incorrectly mapped and the belt speed was calculated to be different from the nominal speed of 4m/s. A similar problem arises when the encoder wheel has damaged spokes resulting in missing pulses being generated by the proximity sensor.

A useful technique which can be used to diagnose such problems is to plot a histogram of the time between consecutive pulses. Since, under normal operation, the belt is moving at a constant speed, the histogram should exhibit a single peak with a time between pulses that corresponds to the nominal speed of 4m/s, as shown in **Figure 9(a)**. The top plot shows a sequence of evenly spaced pulses, and the bottom plot shows a single peak.

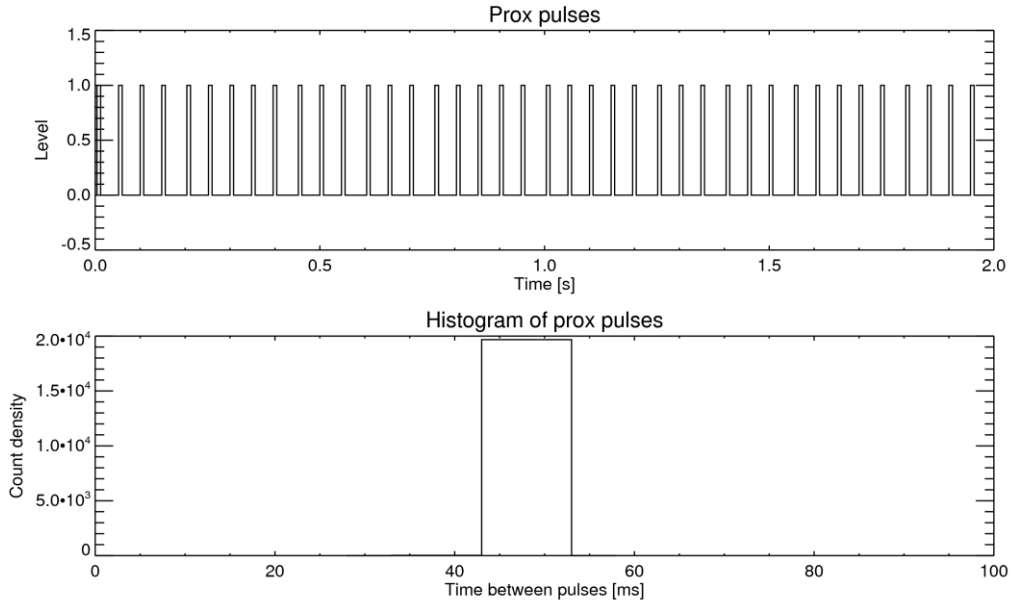

(a)

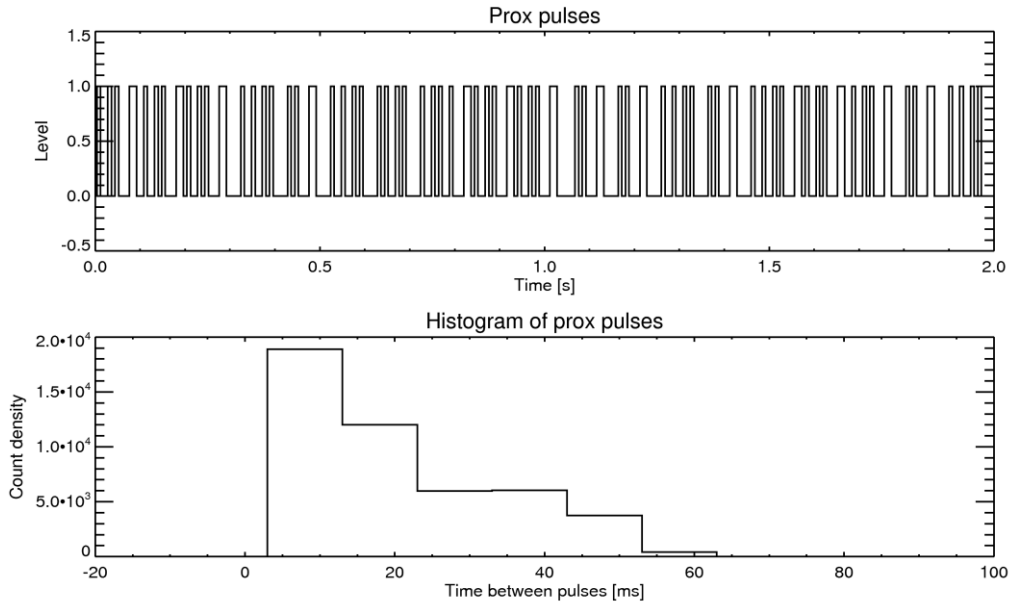

(b)

Figure 9: Histograms of pulses from a proximity sensor: (a) in good working order, and (b) generating erratic pulses implying a problem with the proximity sensor and/or targets.

Conversely, if the pulses are unevenly spaced, as in the case depicted in **Figure 9(b)**, then the corresponding histogram exhibits a multi-peaked distribution. Clearly, if a single spoke on the encoder wheel is consistently missed, then the histogram will display two peaks.

4.3 CASE STUDY: PREVENTATIVE BELT MAINTENANCE AT NEW DENMARK COLLIERY

This section describes the use of DiMI as a tool for belt preventative maintenance at New Denmark Colliery.

Soon after DiMI was installed, in December 2007, Report I was generated and presented to the belt maintenance staff. The belt schematic extracted from this report is shown in **Figure 10(a)**. It was immediately obvious that segments 6, 7 and 9 had a significant number of damages as highlighted by the top oval. Specifically, there were also a significant number of critical alarms being generated by these same segments as highlighted by the bottom oval. This data clearly provided evidence arguing for repair and/or replacement of these segments of the belt.

Belt Schematic from Report I: 1 December 2007

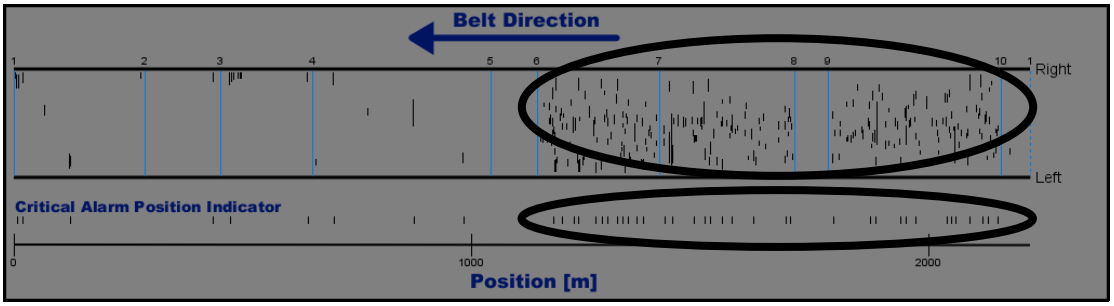

(a)

Belt Schematic from Report II: 17 October 2008

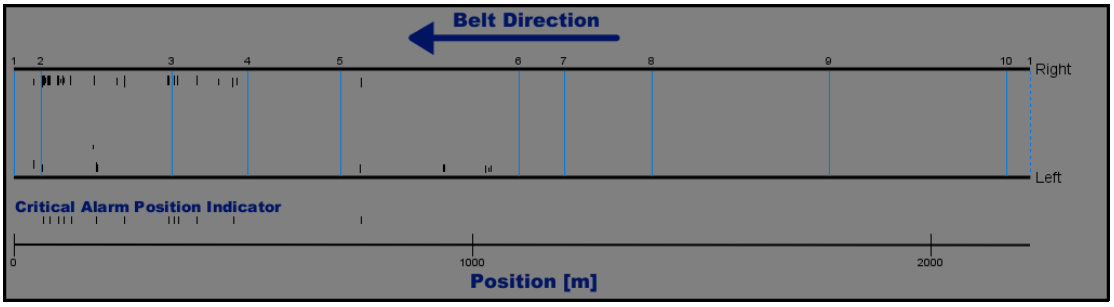

(b)

Figure 10: A comparison of the belt schematics before (Report I) and after (Report II) the segment repair and/or replacement.

After consideration, although segment 8 in **Figure 10(a)** contained few damages, since it was a short segment, it was decided to replace all the belt segments between Splice 6 and 10 in September 2008. During this process, the short segment 8 was removed and an additional short segment (49.5m long) was added.

The schematic extracted from Report II after repair is shown in **Figure 10(b)**. The newly replaced 49.5m segment then became the shortest segment, and hence the reference splice changed. The original shortest segment, appearing on the right hand side of **Figure 10(a)**, is rotated, and now appears on the left hand side of **Figure 10(b)**.

Besides the number of critical damages that appear in the schematic, a metric used for assessing the damage extent of a belt segment is the Average Event Density, defined as the

number of cord breaks per 100m.

Table 1: A comparison of the Average Event Density for each of the belt segments for the Phase 2 Incline Belt at new Denmark Colliery. There is a significantly high number of cord breaks per 100m in segments 6 to 9 for Report I (1 December 2007).

Segment	Segment Length [m]	Status	Average Event Density [Cord Breaks per 100m]	
			Report I: 1 December 2007	Report II: 17 October 2008
1	287.7	Unchanged	17.4	34.1
2	164.4	Unchanged	6.1	18.3
3	202.4	Unchanged	12.8	0
4	389.5	Unchanged	9.5	5.7
5	101.4	Unchanged	0	0
6	192.2	Shortened	116.7	0
7	387.1	Replaced	99.1	0
8	385.9	Replaced	4.1	0
9	49.5	Replaced	89.5	0
10	59.0	Unchanged	3.2	8.5

A comparison of the segment tables extracted from Reports I & II is shown in **Table 1** above. The Average Event Density exceeds 50 cord breaks per 100m in segments 6, 7 and 9. The number of events in the newly-replaced segments 7 through 9 is now, not surprisingly, zero. However, the damages in the remaining segments still need to be monitored. For example, the Average Event Density in the 287.7m long segment has increased from 17.4 to 34.1.

Segment 3, located between splices 3 & 4 in **Figure 10(a)**, had not been replaced but had numerous instances of edge damage, and it can be clearly seen that the Average Event Density has dropped from 9.5 to 5.7. This suggests that the edge damage may have been repaired by removing exposed cords.

The above comparison of reports provides a clear illustration of the effectiveness of DiMI as a continuous belt monitoring system.

5. FUTURE WORK: WAVELET ANALYSIS

5.1 BACKGROUND

When analysing complex time series data sets, Fourier analysis is often used to extract relevant information. The data that is obtained from each of the magnetic sensors is an example of such a time series. However, interestingly, Fourier analysis is not the preferred method for the analysis of such localised, non-periodic data. This fundamental limitation of Fourier analysis makes it an inappropriate choice for efficiently analysing the magnetic fringing field data generated by splices and cord damages as these data display characteristic pulse-like behaviour. A more appropriate technique is to use wavelet analysis[0] which has for some time now been recognised as being more useful to analyse signals that have localised structure in time or space such as seismic echoes, fingerprint images and image compression as formulated in the JPEG 2000-standard. Interestingly, a by-product of this wavelet analysis is that the results make the magnetic data easier to understand since they are more directly related to the size, number of cord breaks and position of the cord damages than the rather more confusing bipolar structure of the raw magnetic signals. It is also found that wavelet

filtering makes the data more immune to (quasi-periodic) vibration and makes the choice of thresholds less critical.

5.2 BELT VIBRATIONS

A fairly problematic issue identified with the New Denmark and some other DiMI installations is excessive belt vibration. These effects show up in the magnetic images as repeated vertical stripes corresponding to a frequency of ~8Hz as shown in **Figures 6 & 7** above. Although fairly recognisable by a human observer, this results in a low signal-to-noise ratio (S/N) that reduces the reliability of the identification of splices and damages.

Clearly, it is preferable to optimise the mechanical configuration to minimise the oscillations. Various configurations of calming rollers were tried, and constraining the belt to be tensioned above and below straight idlers was fairly successful. Even though mechanical solutions can be implemented, their effectiveness differs from site to site. Therefore, signal processing needs to be considered, and in particular, wavelet filtering has been shown to be useful.

The vibration problem can be reduced by convolving the magnetic signal with a suitable wavelet function. **Figure 11** shows a plot through a damage where the belt oscillations appear clearly on either side of the damage giving a relatively low S/N of ~4. After convolving the magnetic data with a wavelet, the damage appears more clearly as shown in **Figure 11(b)** with a S/N of ~34. The noise components due to the quasi-sinusoidal mechanical oscillations have a structure very different from the single pulse asymmetric shape of the fringing field, and hence the wavelet filter succeeds in efficiently enhancing the S/N.

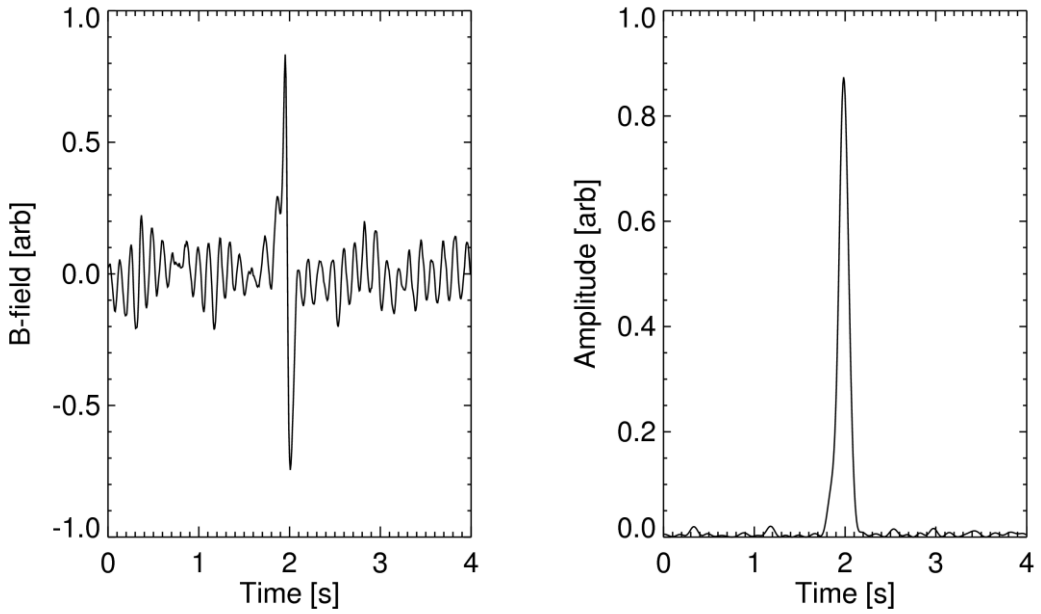

Figure 11: (a) Plot of the *z*-component of the magnetic field, B_z, just above a broken cord in a conveyor belt. The fringing field at the break has the characteristic bipolar structure, however, here sinusoidal oscillations are also seen due to belt vibration giving a fairly low S/N of ~4. (b) After the convolution of the magnetic data with a wavelet function, the damage is clearly visible as a single peak with the noise components being highly attenuated and an improved S/N of ~34.

5.3 THRESHOLD CALCULATION

Another problem that has been experienced is the task of selecting a suitable threshold for locating the splices. After capturing the magnetic data, it is necessary to analyse the time

series data, looking for all peaks that exceed a certain percentage of the maximum value. The amplitude of the magnetic signals depends on a number of factors, including the diameter of the cords, cord pitch, and the sensor-belt and magnet-belt separations. Thus, on commissioning DiMI at a particular site, it is necessary to empirically determine a threshold parameter which is used to identify the splices. In practice, this threshold result is used as a primary characteristic, and other parameters of the magnetic splice such as its elongated shape and oblique orientation are also used to help to unambiguously identify a splice.

In the particular belt data shown in **Figure 12**, the correct number of splices (in this case, 7) is obtained over a relatively narrow threshold range of 20% to 50%, shown by the dashed curve when the raw magnetic data is used. Below 20%, some of the vibration and/or noise peaks are misidentified as being splices leading to a number in excess of the correct number being found. If the threshold value is above 50%, then some of the splices are missed leading to the total number of identified splices being less than 7. If, however, the wavelet filter is applied, then the correct number of splices is found over a much larger range of threshold values from about 1% to 60%. This technique makes the determination of the correct threshold in the field very much less critical and less susceptible to errors due to variations in magnetic field above the splices.

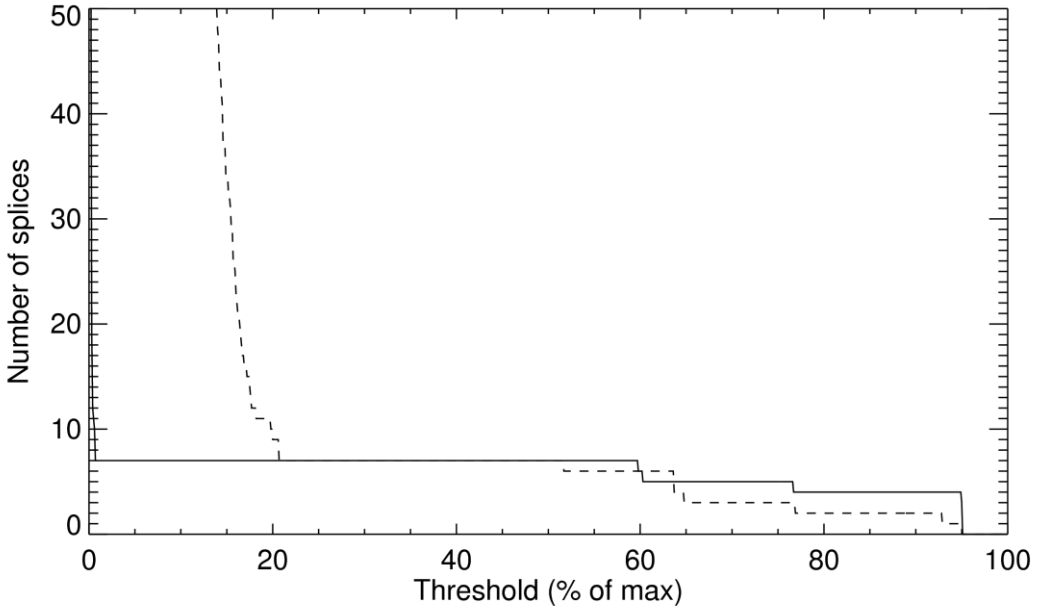

Figure 12: Determination of the number of splices in a belt by applying a threshold to the raw magnetic data (dashed) and the wavelet-filtered data (solid). The correct number of splices (7, in this case) is found over a very much larger range of the threshold parameter if the magnetic data is wavelet-filtered.

6. SUMMARY AND CONCLUSIONS

Following an initial development in the laboratory, the DiMI magnetic imaging technology has now being commissioned at a number of sites around the world. Useful feedback has been received from end users. The hardware has proven to be reliable, and internet connectivity has been successfully used to apply a number of incremental software upgrades.

The use of DiMI as a belt maintenance tool has been demonstrated by comparing segment magnetic data before and after repair and/or replacement at the New Denmark Colliery. Implementing this methodology ensures that belt users can effectively plan their maintenance schedule in order to optimise belt lifetimes.

In addition, this paper has also described how wavelet analysis can be used to discriminate against the effects caused by mechanical belt flap oscillations and also increase the reliability

of identifying the splices in the magnetic imaging data. It is anticipated that some sort of filtering (possibly, wavelet) will be implemented in future software revisions.

7. REFERENCES

[1] Alport MJ, Fourie JH, Basson JF, Padayachee T; "Condition Monitoring of Fabric-Reinforced Conveyor Belting using Digital X-ray Imaging"; Beltcon 13 International Materials Handling Conference, Mintek Conference Centre, 3-4 August 2005, Strijdom Park, Johannesburg, South Africa.

[2] Harrison A; "Magnetic detection of air gaps formed at breaks in conveyor belt cards"; US Pat. 4864233 (Filed 1 August 1985).

[3] Alport MJ, Basson JF, Padayachee T; "Digital Magnetic Imaging of Steel Cord Conveyor Belts"; 14th International Materials Handling Conference; 1-2 August 2007; Birchwood Executive Hotel & Conference Centre, East Rand, Johannesburg, South Africa.

[4] South African Provisional Patent Number 2007/00760 (Filed 25 January 2007).

[5] PCT Patents PCT/IB2008/050250, PCT/IB2008/050254, PCT/IB2008/050255 (Filed 24 January, 2008)

[6] Torrence C and Compo G; Bull of Am. Met. Soc; Vol. 79; p61; 1998.

8. ACKNOWLEDGEMENTS

Advanced Imaging Technologies (Pty) Ltd acknowledges financial support received from The Innovation Fund, Department of Science and Technology.

9. AUTHORS' CV'S

Paper to be presented by MJ Alport.

9.1 CURRICULUM VITAE OF MJ ALPORT

Qualifications:

- BSc (Hons) (Physics) 1974, University of Natal, Durban
- MSc (Physics) 1975-1977, University of Natal, Durban
- PhD (Plasma Physics) 1977-1981, University of Iowa (USA)

Experience:

- 1978 → 2000: Visiting scientist at Laboratoire de Mécanique des Fluides, Grenoble, France; University of Groningen, Nuclear Physics Department, KVI; Dept. of Physics, West Virginia University, Morgantown; Dept. of Nuclear Engineering and Engineering Physics, University of Wisconsin, Madison, Wisconsin; Laboratory for Plasma and Fusion Energy Studies, University of Maryland, College Park, MD; Dept. of Physics and Astronomy, University of Iowa, Iowa City, Iowa
- 1981 → present: Associate Professor and Head of the Applied Physics Group. School of Physics, University of KwaZulu-Natal, Durban
- 2004: Founder and MD of Advanced Imaging Technologies

9.2 CURRICULUM VITAE OF JF BASSON

Qualifications:

- BSc (Physics, Mathematics) 1998, University of Natal, Durban
- BSc (Hons) (Physics) 1999, University of Natal, Durban
- MSc (Physics) 2001, University of Natal, Durban
- PhD (Astrophysics) 2003, University of Cambridge (UK)

Experience:

- March 2003 → December 2003: Consulting Physicist for the Applied Physics Group at the University of Natal
- January 2004 → present: Consulting Physicist for Advanced Imaging Technologies

9.3 CURRICULUM VITAE OF AJ FIDDLER

Qualifications:

- BScEng (Electronic Engineering) 2007, University of Natal, Durban

Experience:

- June to July 2007: Vacation work at Advanced Imaging Technologies
- January 2008 → present: Consulting Electronic Engineer for Advanced Imaging Technologies

9.4 CURRICULUM VITAE OF T PADAYACHEE

Qualifications:

- MSc (Applied Physics) 2001, University of Natal, Durban
- BSc (Hons) 1997, University of Natal, Durban
- BSc (Applied Mathematics, Physics) 1996, University of Natal, Durban

Experience:

- 1995 → 1997: Vacation work at DebTech in Johannesburg, mainly in the field of X-ray and Gamma Spectroscopy
- January 1998 → December 1999: Assistant Research Officer at DebTech. Project experience included X- and Gamma-ray Spectroscopy, X-ray Computed Tomography, X-ray Digital Radiography, Neutron Activation Analysis, X-ray Fluorescence and Infrared Reflectance Spectroscopy
- January 2004 → present: Consulting Physicist for Advanced Imaging Technologies

9.5 ADDRESS OF AUTHORS

MJ Alport, JF Basson, AJ Fiddler and T Padayachee

Advanced Imaging Technologies (Pty) Ltd

Suite #307, Private Bag X04, Dalbridge, 4014, South Africa

Tel: +27 (0)31 202-5528

Fax: +27 (0)31 202-5527

e-Mail: alport@ait-sa.com

Web: www.ait-sa.com